2002

Neutron Powder Diffraction Studies of the $La_{0.65}Pb_{0.35}MnO_3$ Perovskite

Camelia Borca
University of Nebraska-Lincoln

Shireen Adenwalla
University of Nebraska-Lincoln, sadenwalla1@unl.edu

Sy-Hwang Liou
University of Nebraska-Lincoln, sliou@unl.edu

Q.L. Xu
University of Nebraska-Lincoln

J. L. Robertson
Oak Ridge National Laboratory

See next page for additional authors

December 2002

ELSEVIER

Materials Letters 57 (2002) 325–329

MATERIALS LETTERS

www.elsevier.com/locate/matlet

Neutron powder diffraction studies of the $La_{0.65}Pb_{0.35}MnO_3$ perovskite

Camelia N. Borca [a,*], S. Adenwalla [a], S.-H. Liou [a], Q.L. Xu [a], J.L. Robertson [b], P.A. Dowben [a]

[a] *Department of Physics and Astronomy, University of Nebraska, Lincoln, NE 68588-0111, USA*
[b] *Solid State Division, Oak Ridge National Laboratory, Oak Ridge, TN 37831, USA*

Received 10 February 2002; accepted 28 February 2002

Abstract

The structure of $La_{0.65}Pb_{0.35}MnO_3$ has been studied by neutron powder diffraction. From the temperature dependence of the lattice parameters, we observe that $La_{0.65}Pb_{0.35}MnO_3$ remains single phase in the temperature interval from 25 to 400 K, with a rhombohedral ($R\bar{3}c$) structure. The collinear Mn spins suffer a thermally driven reorientation transition close to the Curie temperature, as obtained from powder samples (using neutron diffraction) and from thin films [using ferromagnetic resonance (FMR)]. The reorientation transition may indicate the presence of *local* Jahn–Teller (JT) lattice distortions, which are prevented from developing with long-range order in the $R\bar{3}c$ crystal structure.

Keywords: Perovskites; Crystal structure; Neutron diffraction; Ferromagnetic resonance; Jahn–Teller distortions; Spin reorientation transition

A strong interplay between structure, magnetism and electronic transport has been observed in the ''colossal'' magnetoresistance (CMR) manganese oxides crystallizing in the perovskite structure [1,2]. One common approach for determining the structure of manganese perovskite materials has been powder neutron diffraction [2,3]. In this paper, we focus on determining the details of the crystalline structure of $La_{0.65}Pb_{0.35}MnO_3$, a manganese oxide compound expected to exhibit many of the properties of the heavily studied $La_{0.65}Sr_{0.35}MnO_3$ but less investigated in literature due to sample fabrication difficulties. The experimental results have shown that this Pb-doped system exhibits a Curie temperature of 355 K in the polycrystalline form, with an MR value as high as 50% (at 5.5 T) at 330 K in thin film samples [4].

Our neutron experiments were performed using the HB-4 high-resolution powder diffractometer at the High Flux Isotope Reactor (HFIR) at Oak Ridge National Laboratory. The HB-4 diffractometer has an array of 32 detectors and the available scattering angle is between 11° and 135°. When operated at a wavelength of 1.5 Å (using a Ge (115) monochromator), the maximum wave vector, Q ($=4\pi/\lambda\sin\theta$), that can be reached is ~ 9.07 Å^{-1}.

The polycrystalline sample studied in this experiment was synthesized using standard ceramic methods. The bulk magnetization, resistivity and magnetoresistance are all consistent with previous results [5] ob-

* Corresponding author. JILA, University of Colorado, 440 UCB, Boulder, CO 80309-0440, USA. Tel.: +1-303-492-1265; fax: +1-303-492-5235.

E-mail address: cborca@jilau1.colorado.edu (C.N. Borca).

0167-577X/02/$ - see front matter
PII: S0167-577X(02)00785-1

tained on $La_{0.65}Pb_{0.35}MnO_3$. Fig. 1 shows the result of a full Rietveld analysis at room temperature. The solid line in Fig. 1 indicates the calculated intensities using the GSAS Rietveld analysis software [6]. The initial values used in our refinement of the nuclear structures of $La_{0.65}Pb_{0.35}$ MnO_3 were taken from the atomic parameters reported by Ref. [7]. The neutron diffraction patterns at various temperatures were obtained by merging the data from low and high angle scans of the bank of 32 detectors. The beginning of the high angle scan overlaps the end of the low angle scan. Because the data collected above $T = 300$ K contains scattering from the Al sample can, Al was included in the refinements as a separate phase. We find that the compound has a rhombohedral structure at all temperatures investigated, with the $R\bar{3}c$ space group. The goodness of each fit is given by the weighted profile factor R_{WP} [8]. Because of the Mn magnetic form factor, magnetic contributions to Bragg reflections at $2\theta \geq 60°$ are essentially negligible, even at the lowest temperature, where the magnetic Bragg scattering is at its greatest. Only one pure magnetic Bragg reflection was identified at $2\theta = 31.61°$, attributed to the (Mn-Mn) magnetic structure factor, which corresponds to the (110) planes. The results of one refinement I_{obs}, I_{calc} and the difference plot ($I_{obs} - I_{calc}$) for $La_{0.65}Pb_{0.35}MnO_3$ at 300 K are shown in Fig. 1. The fit shown as a continuous line does not include the contribution from the (Mn-Mn) or the (Mn-O) magnetic structure factors. The first and second sets of vertical marks below the profile indicate the positions of Bragg reflections for the rhombohedral ($R\bar{3}c$) and

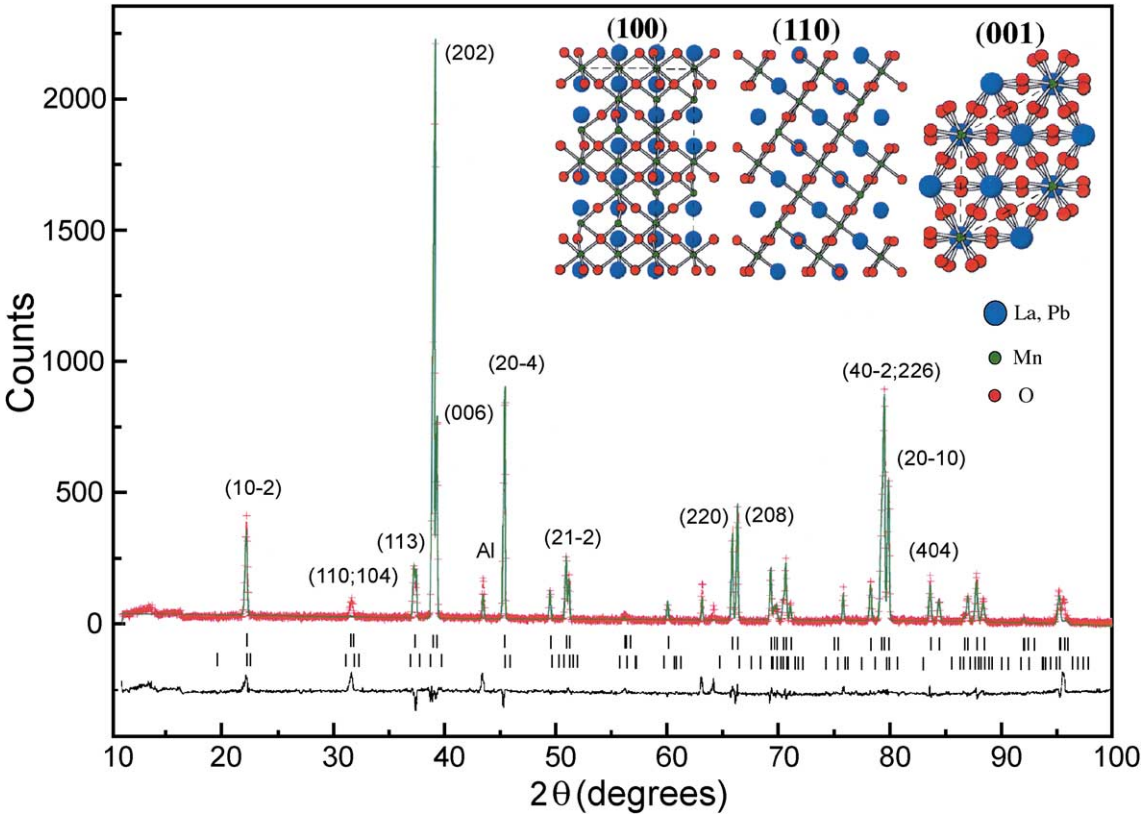

Fig. 1. Rietveld refinement of the neutron powder diffraction pattern of $La_{0.65}Pb_{0.35}MnO_3$ at 300 K. The first and second sets of vertical marks below the profile indicate the positions of Bragg reflections for the rhombohedral ($R\bar{3}c$) and orthorhombic (*Pnma*) structures, respectively. The major reflections are labeled with the rhombohedral indices. The curve at the bottom is the difference between the observed (dots) and the calculated (continuous line) intensities for the rhombohedral structure. The inset shows the unit cell projections along (100), (110) and (001) directions.

orthorhombic (*Pnma*) structures, respectively. As can be clearly seen, the only possible fit to the data is obtained using the rhombohedral structure, in agreement with the results obtained for the $La_{0.7}Sr_{0.3}MnO_3$ compound [8]. The inset in Fig. 1 shows the main projections of the unit cell, (100), (110), and (001), respectively. Table 1 summarizes the lattice parameters, atom positions and bond lengths at five different temperatures. The lattice parameters found at 25 K for our sample [$a = 5.5068$ (2) Å, $c = 13.3401$ (4) Å] are close to other nominal $x = 0.35$ compounds (with different dopants) reported in the literature [8]. The $R\bar{3}c$ rhombohedral phase can only accommodate MnO_6 octahedra with one Mn-O bond length at a given temperature, as compared to the $La_{1-x}Ca_xMnO_3$ compound, which has a *Pnma* symmetry that allows two Mn-O bonds for almost all x values [2,3].

We next compare the (110) and (006) reflections that correspond to projections of the magnetic moment vector onto the *ab* plane and *c* axis, respectively. We compare the integrated intensities of the (110) and (006) peaks after subtracting the nonmagnetic contributions only for the (006) peak. The ratio of these two peaks is related to the tilt angle of the magnetic moment from the rhombohedral *c*-axis as shown in the following relations:

$$I(006) \propto |M|^2 \sin^2 \theta,$$

$$I(110) \propto |M|^2 \cos^2 \theta,$$

$$\frac{I(006)}{I(110)} = K \tan^2 \theta,$$

where $|M|$ is the amplitude of the magnetic moment vector, θ is the tilting angle from the *c* axis, and K is a constant. As can be seen in Fig. 2, the resulting tilt angle reaches a maximum value at 300 K then drops to 45° at 320 K. Above $T_C = 355$ K, the refinements of the tilt angles resulted in large uncertainties due to very weak magnetic peak intensities. The (110) peak intensity decreases faster than the (006) intensity as the temperature approaches T_C. Therefore, the tilt angle values near T_C are close to 90°.

An additional confirmation of the spin reorientation transition, found from neutron diffraction measurements, has been obtained on $La_{0.65}Pb_{0.35}MnO_3$ thin films using ferromagnetic resonance (FMR) technique [9]. The temperature dependence of the angle Φ, representing the average orientation of the electronic spins in the plane of the film, is plotted in Fig. 2. Note that the different tilt angles of the magnetic moments are not measured with respect to the same crystallographic axis. X-ray diffraction shows that the thin films are oriented perpendicular to (100) direction, assuming a cubic structure. This (100) cubic plane corresponds to the (10-2) plane in the rhombohedral structure, indicating the same Mn-Mn interlayer spacing of 3.86 Å. The (100) cubic plane and the (10-2) rhombohedral plane make an approximate angle of 54° with the rhombohedral *c*-axis. Therefore, the tilting angles of the spins show different values in Fig. 2. The presence of a moment reorientation transition is obvious in the temperature dependence of the two different tilting angles close to the Curie temperature, where both show an anomalous drop followed by a tendency to recover the low temperature values.

The temperature dependence of the magnetic moment tilt angle obtained from neutron diffraction measurements is similar to results found recently in

Table 1
Refined structural parameters from Rietveld analysis of $La_{0.65}Pb_{0.35}MnO_3$, space group $R\bar{3}c$, with Mn on (0,0,0), La/Pb on (0,0,0.25) and O on (*x*,0,0.25)

Parameter	$T = 25$ K	$T = 100$ K	$T = 200$ K	$T = 300$ K	$T = 400$ K
a (Å)	5.5068 (2)	5.5074 (6)	5.5110 (5)	5.5164 (3)	5.5226 (2)
c (Å)	13.3401 (4)	13.3478 (6)	13.3676 (5)	13.3901 (9)	13.4098 (4)
O-*x* (Å)	0.5436 (2)	0.5428 (1)	0.5419 (3)	0.5421 (4)	0.5408 (4)
O-*B* (Å^2)	0.0108 (9)	0.0122 (3)	0.0146 (8)	0.0157 (1)	0.0185 (7)
Mn-*B* (Å^2)	0.0035 (7)	0.0042 (4)	0.0057 (4)	0.006 (1)	0.0059 (8)
La/Pb-*B* (Å^2)	0.0058 (1)	0.0071 (7)	0.0099 (4)	0.0079 (9)	0.0141 (4)
Mn-O bond (Å)	2.1232 (3)	2.1239 (5)	2.1261 (7)	2.1287 (5)	2.1314 (8)
R_{WP}	5.091	4.873	4.268	3.428	4.013

Numbers in parentheses are statistical errors of the last significant digit. R_{WP} is the weighted profile factor (see Ref. [8]) and *B* is the isotropic temperature factor.

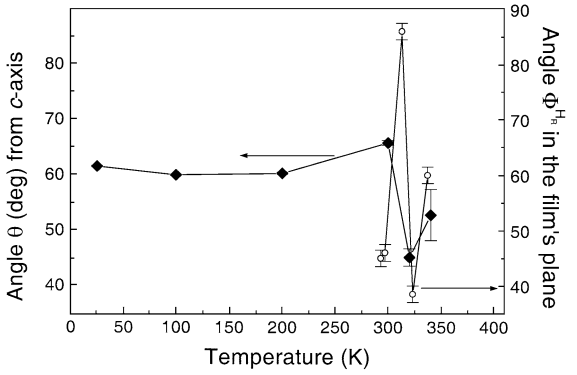

Fig. 2. Temperature variation of the tilting angle (θ) between the Mn-spins and the c-axis of the rhombohedral structure $R\bar{3}c$ (left axis) and the temperature dependence of angle Φ that represents the average orientation of the electronic spins with respect to the in-plane (100) cubic axis (right axis). Angle θ was obtained from neutron diffraction results, while angle Φ was extracted from ferromagnetic resonance results.

$La_{2-2x}Sr_{1+2x}Mn_2O_7$ ($x=0.3$) bilayer manganite [10]. In Ref. [10], the abrupt change of the tilt angle is correlated with a magnetostrictive effect on the c-axis and thus to a variance of the Mn-O bond distances. It is necessary to mention that the symmetry constraints for a $R\bar{3}c$ structure do not allow two different oxygen positions that could result in two Mn-O bonds and the presence of Jahn–Teller (JT) distortions. In spite of the excellent Rietveld fitting results, recent experiments performed on $La_{1-x}Sr_x$ MnO_3 using neutron diffraction to measure the pair density function for Mn-O bond indicate that the local atomic structure significantly deviates from the average structure, and a *local* Jahn–Teller distortion persists even when the crystallographic structure shows no JT distortion [11]. Our results are in agreement with Jahn–Teller distortions found in La_{1-x} Sr_xMnO_3 by recent extended X-ray absorption fine structure (EXAFS) measurements [12], high-resolution electron microscopy observations [13] and neutron scattering experiments [11], all of which indicate that JT distortions are *locally* present in the rhombohedral phase ($R\bar{3}c$), beyond $x=0.2$ for La_{1-x} Sr_xMnO_3 [11]. It is likely that the orientation of the local JT distortion varies from site to site in the rhombohedral phase, and the symmetry is maintained only on average.

A small number of Mn atoms, randomly distributed throughout the entire sample, are in the oxidation state III (with an outer electronic configuration of d^4), which is Jahn–Teller active, while the majority of Mn atoms are in the electronic configuration d^3, which is not JT active. At temperatures well below T_C, more electrons become delocalized in a conduction band, and the manganese atoms become equivalent, leading to the complete disappearance of the Jahn–Teller distortions. Close to the Curie temperature, the Mn^{3+} octahedra become locally JT active and the spins are canted at an average angle with respect to the c-axis corresponding to $R\bar{3}c$ structure. It is possible that the JT distortions prevail above the Curie temperature, as was recently investigated in FMR measurements [9]. It also known that larger dopant atoms, such as Sr and Pb, introduce a higher degree of disorder, and the system adopts a rhombohedral structure with apparently no Jahn–Teller distortions. Weak Jahn–Teller distortions may be present in the Pb-doped perovskite only on a *local* scale, similar to the distortions found in the Sr-doped manganese perovskites [11].

In summary, the sample of $La_{0.65}Pb_{0.35}MnO_3$, has been shown to adopt a rhombohedral crystalline structure with the $R\bar{3}c$ space group. In the metallic ferromagnetic phase, close to the Curie temperature, the Mn spins experience a thermally driven reorientation transition. The moment reorientation is consistent with the presence of *local* Jahn–Teller distortions. Clearly, different metal dopants introduce various degrees of disorder in the CMR perovskites, which affect the structure, magnetic correlations and transport properties.

Acknowledgements

The authors are grateful to B.C. Chakoumakos and P. Dai for advice with the GSAS fitting program and for helpful discussions. This research was supported by the NSF (grant DMR-98-02126). Oak Ridge National Laboratory is managed by UT-Battelle LLC under contract DE-ACOS-00OR22725 for the U.S. Department of Energy.

References

[1] A.P. Ramirez, J. Phys., Condens. Matter 98171 (1997) 8171.
[2] M. Imada, A. Fujimori, Y. Tokura, Rev. Mod. Phys. 70 (1998) 1039.

[3] P. Dai, et al., Solid State Commun. 100 (1996) 865;
P. Dai, et al., Phys. Rev., B 54 (1996) R3694.
[4] Q.L. Xu, M.T. Liu, Y. Liu, C.N. Borca, H. Dulli, P.A. Dowben, S.-H. Liou, Mater. Res. Soc. Symp. Proc. 602 (2000) 75.
[5] R. Mahediran, R. Masesh, A.K. Raychaudhuri, C.N.R. Rao, J. Phys., D. Appl. Phys. 28 (1995) 1743.
[6] A.C. Larson, R.B. Von Drele, GSAS—General Structure Analysis System, Los Alamos National Laboratory, 1986.
[7] P.M. Woodward, Acta Crystallogr. B53 (1997) 32.
[8] S.J. Hibble, S.P. Cooper, A.C. Hannon, I.D. Fawcett, M. Greenblatt, J. Phys., Condens. Matter 11 (1999) 9221.
[9] M. Chipara, S. Adenwalla, S.-H. Liou, M.T. Liou, Q.L. Xu, C.N. Borca, et al., in preparation.
[10] E.-O. Chi, K.-P. Hong, Y.-U. Kwon, N.P. Raju, J.E. Greedan, J.-S. Lee, N.H. Hur, Phys. Rev., B 60 (1999) 12867.
[11] D. Louca, T. Egami, E.L. Brosha, H. Röder, A.R. Bishop, Phys. Rev., B 56 (1997) R8475;
B. Dabrowski, X. Xiong, Z. Bukowski, R. Dybzinski, P.W. Klamut, J.E. Siewenie, J. Shaffer, C.W. Kimball, Phys. Rev., B 60 (1999) 7006.
[12] T.A. Tyson, et al., Phys. Rev., B 53 (1996) 13985;
C.H. Booth, et al., Phys. Rev., B 54 (1996) R15606.
[13] M. Herview, et al., Phys. Rev., B 53 (1996) 14274.